Semnan University

Journal of Heat and Mass Transfer Research

Journal homepage: https://jhmtr.semnan.ac.ir

ISSN: 2383-3068

Research Article

Numerical Simulation of Atmospheric Water Harvesting Using an Innovative Adsorption-Based Device

Zahra Piryaei [a], Aryan Jouneghaninaseri [a], Maryam Karami [a]*

[a] *Department of Mechanical Engineering, Kharazmi University, Tehran, Iran*

ARTICLE INFO

Article history:

Received: 2024-12-10

Revised: 2025-02-09

Accepted: 2025-03-02

Keywords:

Adsorption-based atmospheric water harvesting (ABAWH);

Water harvesting;

Moisture adsorption;

Silica gel;

Numerical simulation;

ABSTRACT

Water scarcity in arid areas is one of the serious problems of the world today. The inefficiency of traditional water production methods such as refrigeration cycles and the lack of access to water wells in these areas have urged researchers to study methods of harvesting water from air humidity using moisture sorbents. This study aims to numerically simulate the process of water harvesting inside the sorbent bed of an innovative adsorption-based atmospheric water harvesting system using silica gel sorbent in an arid area. The proposed design is an active system consisting of two sorbent beds composed of sinusoidal channels, in which the adsorption/desorption processes are quasi-continuously performed. The governing equations on the system performance are derived and solved using the finite difference method. The proposed design can perform 12 cycles of distilled water production in 12 hours daily, yielding a water production of 0.166 mL/kJ and 31670 mL per unit area of the inlet cross-section of the sorbent bed. The average rate of distilled water production by this design is 19440 mL/h, which is about 30% higher than the production rate of a mono-cycle active system and 20% higher than an active system with one sorbent bed.

1. Introduction

Today, more than one billion people around the world lack access to safe drinking water. The problem of water shortage has encouraged scientists to find different ways to produce water. One of the newest methods is harvesting water from the air since there is a significant volume of water molecules in the atmosphere, which can serve as a viable and safe source of fresh water. This method of water extraction is environmentally friendly, as the moisture drawn from the air is replenished naturally through the earth's hydrological cycle [1].

Harvesting water from air moisture can be carried out by different methods. The most common method is to use the refrigeration cycle and bring the air temperature to the dew point. The main disadvantage of this method is its low efficiency in arid areas with relative humidity less than 40%. For this reason, scientists have proposed an innovative method to extract air moisture, which is known as adsorption-based atmospheric water harvesting (ABAWH). Using this technology, the air moisture is adsorbed by sorbents and released when these sorbents are heated; this moisture is then liquified in a condenser [2].

* **Corresponding author.**
E-mail address: karami@khu.ac.ir

Cite this article as:
Piryaei, Z., Jouneghaninaseri, A. and Karami, M., 2025. Numerical Simulation of Atmospheric Water Harvesting Using an Innovative Adsorption-Based Device. *Journal of Heat and Mass Transfer Research*, 12(2), pp. 377-391.
https://doi.org/10.22075/JHMTR.2025.36216.1657

The phenomenon has been previously seen in desiccant wheels used for air dehumidification [3]. This method is particularly practical for arid areas that face the greatest water scarcity and have extremely low dew point temperatures due to low humidity [4]. ABAWH can reduce energy consumption by significantly increasing the dew point temperature in these areas [5-8].

Although multiple techniques have been suggested to supplement potable water such as solar desalination and membrane distillation [9-11], unlike the ABAWH technique, most of them rely on access to water sources and extensive infrastructure, making them inapplicable in remote and water-scarce regions. ABAWH systems are classified into different types based on sorbent material, active and passive design, continuous and discontinuous operation, and number of cycles (mono-cycle and multi-cycle). Several sorbents have been proposed so far, including silica gel, metal-organic framework (MOF), calcium chloride ($CaCl_2$), etc. If the adsorption/desorption processes are carried out naturally, during 24 hours, the system is known as passive. In active systems, a forced airflow induced by a fan passes through the sorbent bed. In discontinuous systems, when the adsorption process is in progress, the desorption process does not occur, and vice versa. In the continuous system, both adsorption and desorption processes are simultaneously performed and there is no interruption in water production.

During the last few years, numerous experimental studies have been conducted on the ABAWH systems. Kim et al. [12] proposed a passive and discontinuous design in which only one complete cycle (including the adsorption and desorption process) is carried out per day. The sorbent used in this study is the MOF-801 powder layered on a metal mesh plate. The proposed design achieves a water production rate of 340 mL/m^2 (per unit area of the sorbent layer) in each cycle under the summer weather conditions of the Arizona desert. In another design by Kim et al. [13] with an almost similar structure, the system can produce 300 mL/kg of water by using 1.34 g of MOF-801. Hanikel et al. [14] were able to produce 1300 mL/kg at the temperature of 27°C and relative humidity of 32% by using MOF-303 in an active and discontinuous system with a layered sorbent bed. Fathieh et al. [15] reported that by using a passive and discontinuous design with MOF-801, 100 mL/kg of water is generated, which is doubled using MOF-303. In the passive and discontinuous design proposed by Ejeian et al. [16], a bed made of $LiCl/MgSO_4$/ACF and a cone-shaped condenser filled with PCM, which maintains the temperature constant during condensation, are used. This design leads to generating 920 mL/kg at a relative humidity of 35%.

Sleiti et al. [17] used orange silica gel as a sorbent for a passive and discontinuous device. The results of their tests show that the device can produce 159 mL of water per day per kilogram of silica gel at a temperature of 22°C and a relative humidity of 60%. The research conducted by these researchers showed that the thinner the sorbent bed, the higher the efficiency of the system and the higher the water production rate. By placing orange-colored silica gel in a system similar to a solar pond, Kumar et al. [18] showed that water is generated at a rate of 98 mL/kg at a relative humidity of 80% and a temperature of 25°C. In another passive and discontinuous design by Kumar et al. [19], silica gel is placed on a metal mesh and placed inside a sloping glass chamber, which is open at night and closed during the day. The produced water in this study was reported to be 200 mL/day. Essa et al. [20] achieved a water production of 400 mL/m^2 by using a double-slope solar basin containing silica gel with a depth of 1.5 cm inside a passive and discontinuous system. Srivastava et al. [21] used a solar concentrator plate to increase the heat transferred to the sorbent chamber of a passive and discontinuous system. In this research, three sorbents LiCl/sand (CM-1), $CaCl_2$/sand (CM-2), and LiBr/sand (CM-3) were used, which resulted in the generation of distilled water at the rate of 90 mL/day, 115 mL/day, and 73 mL/day, respectively. Another passive and discontinuous device proposed by Elashmawy et al. [22] was a tubular solar still filled with $CaCl_2$ and connected to a parabolic solar concentrator, which yielded 510 mL/kg. Fathy et al. [23] designed a passive solar-powered foldable apparatus composed of a cotton cloth impregnated with $CaCl_2$ solution that led to a water production rate of 750 mL/day. Wang et al. [24] also used the $CaCl_2$ solution in a passive system and 2890 mL/m^2 of water was generated per day under 70% relative humidity. In another passive and discontinuous design proposed by LePutin et al. [25], instead of one sorbent layer, two sorbent layers containing zeolite and two condensers, which are placed under each other, are used. In such a system, the heat released as a result of condensation from the first condenser leads to the desorption of the second layer and the system efficiency increases. Using this design, 60 mL of water per cycle at the temperature of 25°C and relative humidity of 35% is generated. Bio-sorbents have also attracted attention in recenet years. In a study by Raveesh et al. [26], an eco-friendly composite sorbent (SBAC/$CaCl_2$) derived from sugarcane bagasse was developed, demonstrating a higher water uptake capacity than silica gel and showing promising potential for water harvesting.

The passive and continuous design proposed by Li et al. [27] used a rotating cylinder to reverse the adsorption and desorption processes with the aim of performing them simultaneously. The results showed that water at a rate of 1600 mL/kg is generated using 2.93 g of HSC-LiCl in an environment with 60% relative humidity.

Most of the above-mentioned studies have used a thin bed to place the sorbent, and in fact, the sorbent bed is a plate with a small thickness. In the research conducted by Wang et al. [28], wavy plates in sinusoidal form were used to increase the contact surface of the sorbent containing ACF-LiCl and air. This active and discontinuous system can hold 70 kg of sorbent material in the sorbent bed and the device can generate 38500 mL of water. In another study by Wang et al. [29], the previous system was used without energy storage. The results indicated that 9000 mL of water was generated using 40.8 kg of ACF-LiCl.

In a recent experimental study by Agrawal et al. [30], a novel system was introduced, incorporating a solar air heater encapsulated with PCM to enable continuous water generation beyond daylight hours when the primary heat source (solar radiation) is unavailable. The results demonstrate a water extraction rate of 4100 mL/day by using 20 kg of sorbent. In a similar study by these researchers, the water harvesting potential was assessed without the use of PCM for heat storage, yielding 1840 mL/day with 15 kg of sorbent [31]. Another similar research utilized almost the same device but with 12 kg of Jute/$CaCl_2$ as the sorbent, showing a water yield of 5850 mL/day [32].

As the literature review shows, despite significant advancements in atmospheric water harvesting technologies, most prior studies have primarily focused on optimizing sorbent material performance rather than enhancing the overall thermodynamic and structural efficiency of these systems. Furthermore, all of these studies have been conducted experimentally, with limited theoretical and numerical investigations into the adsorption-desorption process. These studies have mainly focused on passive and discontinuous designs, leaving active and particularly continuous systems largely unexplored.

This study introduces a novel approach by investigating the feasibility and water production potential of an active and quasi-continuous ABAWH system through numerical simulation, offering a detailed numerical perspective on the dynamic adsorption-desorption process within a dual-bed configuration. The proposed system integrates two sorbent beds operating in an alternating mode to achieve near-continuous water production, a design aspect that has received minimal attention in previous studies. Silica gel is used as the sorbent due to its abundance and affordability, ensuring practical applicability. This study facilitates further investigations by presenting a detailed numerical approach, providing a foundation for future advancements in the theoretical understanding and design of adsorption-based water harvesting technologies.

2. Materials and Methods

2.1. System Structure

The proposed design is an active ABAWH system that has a quasi-continuous operation. In this design, two separate sorbent beds are used rather than one. The energy source for heating the inlet air can be a solar collector, a heating element, or a combination of them, which is installed at the inlet of the sorbent bed. The sorbent beds are composed of a large number of sinusoidal channels placed on top of each other forming two rectangular beds with a depth of 20 cm and an inlet cross-sectional area of 1.225 m^2. The sinusoidal channels used in the sorbent bed are commonly employed in the air conditioning industry, especially in desiccant wheels due to their enhanced surface area which results in improved mass and heat transfer between air and sorbent layers. Two air-cooled condensers are also considered, which are activated or deactivated depending on whether the adsorption process is in progress or the desorption process as shown in Fig. 1.

In an attempt to establish nearly continuous operation, the air is sucked by the fans in both beds at the same time. In other words, adsorption and desorption occur in both beds separately. While one bed adsorbs moisture, the other undergoes desorption. Once these processes are complete, the roles reverse (Fig. 1). Thus, each water harvesting cycle consists of one full adsorption process and one full desorption process. The next cycle begins when the mentioned reversal takes place. However, it should be noted that the continuous operation of the system depends on the kinetics of each process. There would not have been any interruption in the water production cycle if the time required to perform these two processes had been the same. However, due to the differences in their chemical characteristics, it is difficult to perform them simultaneously, and there will always be a discontinuity in the system performance. In addition, when the desorption process is completed, the surface temperature of the sorbent layers must be cooled again so that adsorption takes place properly.

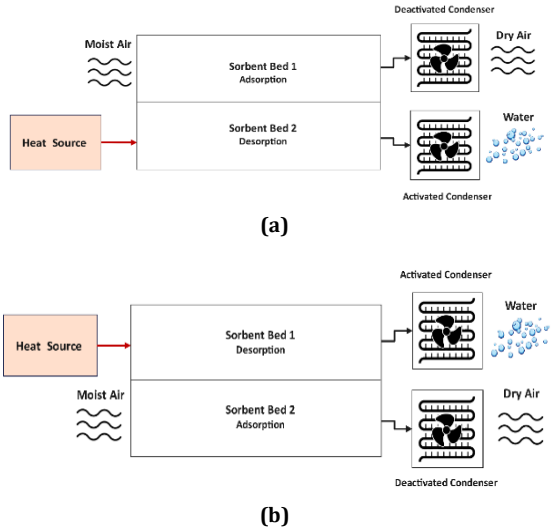

Fig. 1. Schematic representation of the proposed active ABAWH system for (a) the base cycle and (b) the reversed cycle

2.2. System Modeling

2.2.1. Governing Equations

The proposed sorbent bed, where silica gel is layered on sinusoidal plates, is shown schematically in Fig. 2. As air flows through the sorbent layers, moisture and heat transfer take place. For the simplicity of calculations, the mass and energy conservation equations are written discretely for an intermediate element (channel), whose output properties can be considered as an average for the entire outlet section.

Considering each element specified in Fig. 2 as a control volume, the governing equations for this computational domain can be derived using the laws of conservation of mass and energy.

The following assumptions are considered for modeling:

1. The airflow along the bed is one-dimensional and laminar.
2. All layers of the sorbent bed have the same characteristics.
3. The sorbent bed is completely insulated.
4. The inlet cross-section of each element has a sinusoidal shape with a width b=3.5 mm and a height a=1.75 mm. Also, the length of the bed is 20 cm.
5. The thickness of the sorbent layer is about 0.3 mm.
6. The porosity ratio is considered equal to 70% [33-35].
7. The heat and mass transfer coefficients as well as specific heat are assumed to be constant along the bed.
8. In all energy conservation equations, kinetic and potential energy changes are neglected.

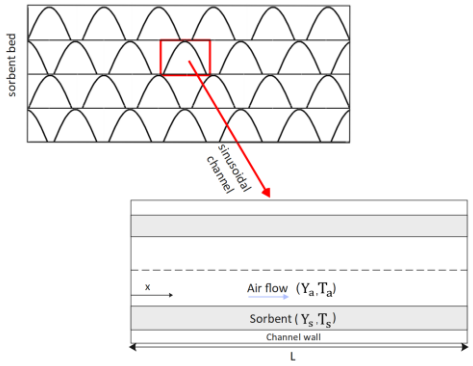

Fig. 2. Computational domain

Considering the one-dimensional control volume in Fig. 2, the mass conservation for the airflow is as follows [33]:

$$\rho_a\left(\varepsilon\left(\frac{\partial Y_a}{\partial t}\right)+u_a\left(\frac{\partial Y_a}{\partial x}\right)\right)=\alpha h_m(Y_s-Y_a) \quad (1)$$

where h_m is the convective mass transfer coefficient, which is calculated using the following relation [36] :

$$h_m=\frac{h}{c_p\times Le} \quad (2)$$

where h is the convective heat transfer coefficient and Le is the Lewis factor which is equal to 1 for air in this study.

The mass conservation equation for the sorbent bed can be written as [37]:

$$\rho_s(1-\varepsilon)\left(\frac{\partial W}{\partial t}\right)=\alpha h_m(Y_a-Y_s)+\frac{\partial}{\partial x}\left(D_s\left(\frac{\partial W}{\partial x}\right)\right) \quad (3)$$

where D_s is the mass diffusion coefficient. In this study, only the surface diffusion is considered and Knudsen diffusion is neglected. Therefore, the mass diffusion coefficient is calculated as [37]:

$$D_s=\frac{D_0}{\tau}exp\left(-0.974\times10^{-3}\left(\frac{Q_{sor}}{T+273.15}\right)\right) \quad (4)$$

in which D_0 is equal to 1.6×10^{-6} m^2/s.

Considering the first law of thermodynamics in the differential form, the energy conservation equation for the airflow is as follows [33]:

$$\rho_a(C_{pa}+Y_aC_{pv})\left(\varepsilon\left(\frac{\partial T_a}{\partial t}\right)+u_a\left(\frac{\partial T_a}{\partial x}\right)\right)=\alpha h(T_s-T_a) \quad (5)$$

h can be obtained using the Nusselt number (Nu):

$$h=\frac{Nu(k_a)}{D_h} \quad (6)$$

where Nu is obtained as [34]:

$$Nu = \frac{N_{uT} + N_{uH}}{2}$$
$$N_{uT} = 1.1791 \times \left(1 + 2.7701\alpha^* - 3.1901\alpha^{*2} - 1.9975\alpha^{*3} - 0.4966\alpha^{*4}\right)$$
$$N_{uH} = 1.903 \times \left(1 + 0.4556\alpha^* + 1.2111\alpha^{*2} - 1.6805\alpha^{*3} + 0.7724\alpha^{*4} - 0.1228\alpha^{*5}\right) \quad (7)$$
$$\alpha^* = \frac{a}{b}$$

The hydraulic diameter (D_h) is calculated using the following relation [34]:

$$D_h = b \times (1.0542 - 0.4660\alpha^* - 0.1180\alpha^{*2} + 0.1794\alpha^{*3} - 0.0436\alpha^{*4})\alpha^* \quad (8)$$

The energy conservation equation for the sorbent bed is as follows:

$$\rho_s(1-\varepsilon)\left(\frac{\partial\left(C_{ps} + WC_{pl}\right)T_s}{\partial t}\right) = \alpha[h_m(Y_a - Y_s)Q_{sor} + h(T_a - T_s)] + \frac{\partial}{\partial x}\left(k\left(\frac{\partial T_s}{\partial x}\right)\right) \quad (9)$$

where Q_{sor} is the evaporation enthalpy or in other words, the energy required to desorb the moisture trapped in the sorbent layers. This quantity is a function of air temperature [35]:

$$Q_{sor} = 2500 + c_{pv} \times T_a \ \ (kJ) \quad (10)$$

Table 1 shows the thermophysical properties of the materials used in the proposed system.

Table 1. Thermophysical properties of the proposed system's materials

Properties	Value
Sorbent specific heat (c_{ps})	$921\ \frac{J}{kg.K}$
Bulk sorbent density (ρ_s)	$720\frac{kg}{m^3}$
Sorbent thermal conductivity (k)	$0.11417\frac{W}{m.K}$
Liquid water specific heat ($c_{p\,l}$)	$4186\frac{J}{(kg.K)}$
Water vapor specific heat ($c_{p\,v}$)	$1872\frac{J}{(kg.K)}$
Average air density (ρ_a)	$1.1614\frac{kg}{m^3}$
Air thermal conductivity (k_a)	$0.0263\ \frac{W}{m.K}$

To obtain all five unknowns in the governing equations (Eqs. (1), (3), (5), and (9)), a new equation that relates the water uptake capacity of the sorbent (W) to the other unknowns of the problem is needed, which can be derived from the sorbent isotherm diagram. The following empirical equation relates the water uptake capacity of silica gel (W) to the humidity ratio of the sorbent surface (Y_s) [34, 38]:

$$\varphi_s = \sum_{i=0}^{5} a_i W^i \quad (11)$$

where φ_s is the relative humidity of the thin air layer in contact with the sorbent surface. a_i are the constant values obtained from experimental results. By rewriting Eq. (11), the following equation is obtained:

$$\varphi_s = 0.0078 - 0.0576W + 24.2W^2 - 124W^3 + 204W^4 \quad (12)$$

The following relations are utilized to calculate the parameters used in the aforementioned equations [37]:

$$Y_s = \frac{0.622\varphi_W P_{vs}}{P - P\varphi_s} \quad (13)$$

$$ln\left(\frac{P_{vs}}{22087.87}\right) = \frac{0.01}{T + 273.15}(374.136 - T)\sum_{i=1}^{8} F_i(0.65 - 0.01T)^{i-1} \quad (14)$$
$$F_1 = -741.9242 \quad F_2 = -29.7210$$
$$F_3 = -11.55286 \quad F_4 = -0.8685635$$
$$F_5 = 0.1094098 \quad F_6 = 0.439993$$
$$F_7 = 0.2520658 \quad F_8 = 0.05218684$$

Since all equations are time-dependent, the initial conditions should be specified to solve the equations. The initial value of each parameter depends on the assumption applied which can vary depending on the experimental conditions.

In this study, it is assumed that the sorbent is initially saturated and has a water uptake capacity equal to $0.17\ kg_w/kg_s$. The initial capacity was determined through a numerical simulation. Starting with a value of zero, the simulation was run until a steady-state was achieved. At equilibrium with room temperature, the sorbent's ultimate capacity was found to be $0.17\ kg_w/kg_s$. This was also shown in [33, 34]. Therefore, at first, the desorption process is carried out, during which the moisture stored in the adsorbent material is desorbed over time and the moisture content of the passing air increases. Simply put, this study assumes that the sorbent

bed was initially in equilibrium with the ambient air and was completely saturated at the beginning of the desorption process.

The initial and boundary conditions are reported in Table 2, in which the air properties are considered according to the weather conditions of Tehran on a spring day with a relative humidity of 35%. It should be noted that the airflow used for the desorption process is the atmospheric air, which has only undergone simple heating and does not experience humidity change. The sorbent bed boundary conditions are assumed to be insulated due to negligible heat transfer [37, 39].

Table 2. Initial and boundary conditions

Conditions	Value
Air initial temperature	$T_{ai} = 30°C$
Sorbent initial temperature	$T_{si} = 30°C$
Sorbent initial water uptake capacity	$w = 0.17 \frac{kg_w}{kg_s}$
Air initial humidity ratio	$Y_{ai} = 0.0093 \frac{kg_w}{kg_a}$
Inlet air temperature	T_a at x: 0 $= 80°C$
Inlet air humidity ratio	Y_a at x: 0 $= 0.0093 \frac{kg_w}{kg_a}$
Insulated surface for sorbent temperature at inlet	T_s at x: 0 $\frac{\partial T_s}{\partial x} = 0$
Insulated surface for water uptake capacity at inlet	w at x: 0 $\frac{\partial w}{\partial x} = 0$

After the full implementation of the desorption process within a specified time, the last state of the sorbent layer properties (variables of T_s and w) will be their initial condition in the adsorption process since adsorption and desorption take place right after each other. In addition to initial and boundary conditions, parameters such as time and air flow rate have also a significant impact on the results. Desorption generally occurs faster than adsorption. Therefore, the time allocated to these two processes cannot be the same, which leads to a discontinuity in the system performance.

2.2.2. Numerical Simulation

The explicit forward time-centered space (FTCS) finite difference method, a suitable solver with low computational cost, is used in this study as the numerical method. Adsorption and desorption processes are both divided into several time steps, during which Eqs. (1), (3), (5), (9), and (13) are simultaneously solved to compute air and sorbent properties based on the values obtained in the previous step. The computation procedure continues until the considered time period for each process.

To evaluate the grid independence of the simulation results, the effect of three different grids including Grid 1: $\Delta x = 0.01$ m and $\Delta t = 0.001$ s, Grid 2: $\Delta x = 0.02$ m and $\Delta t = 0.001$ s, and Grid 3: $\Delta x = 0.01$ m and $\Delta t = 0.005$ s, on air humidity ratio, is investigated. Fig. 3 indicates that the obtained results are more dependent on the number of time nodes than on the number of spatial nodes. Thus, Grid 1 is selected as the base grid which has 20 spatial nodes and 90000-time nodes. The average difference in the results between the selected grid and the second and third grids is 10% and 0.01%, respectively.

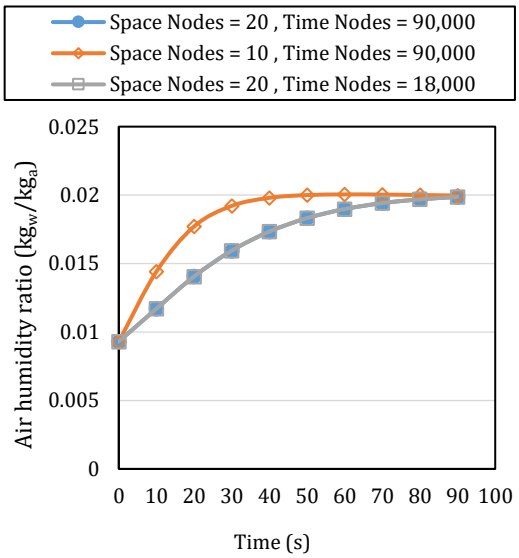

Fig. 3. Grid independency

To assess the validity of the proposed model, the results are compared with those obtained by Kang et al. [33]. For this purpose, the model input data are considered following Kang et al.'s research [33], which are listed in Table 3.

Table 3. Input data for model validation [20]

Parameter	Value	Parameter	Value
$T_{a,p,i}$	30°C	u_a	$2.0 \frac{m}{s}$
$T_{a,r,i}$	70°C	t_p	$90\ s$
$Y_{a,p,i}$	$0.0133 \frac{kg_w}{kg_a}$	f_m	0.5
$Y_{a,r,i}$	$0.0133 \frac{kg_w}{kg_a}$	α	$1630 \frac{1}{m}$
L	$0.2\ m$	ε	0.707

Fig. 4 shows the outlet air and the sorbent surface temperature during the desorption process. As can be seen, the results of the present simulation differ by 9.41% and 5.12% with that of Kang et al. [33], respectively. The reason behind this difference is that Kang et al. [33] neglected temperature and humidity variation along the sorbent bed (x direction), while the present study assumes the sorbent bed properties to be both time and space-dependent.

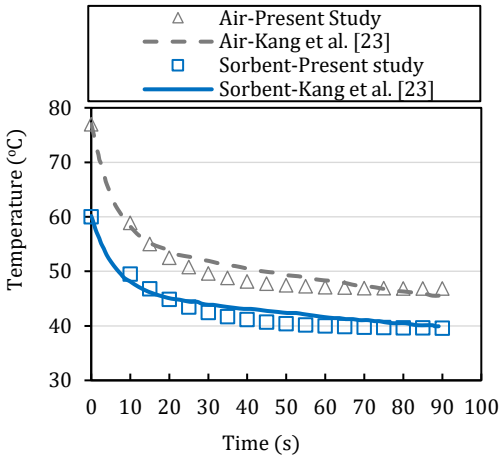

Fig. 4. Outlet air and sorbent surface temperature during the desorption process

2.2.3. Performance Indicators

The initial stage of the water production cycle is moisture adsorption from ambient air by passing it over the sorbent layers. The difference in the moisture content of the passing air at the inlet and outlet of the sorbent bed indicates the amount of moisture adsorbed by the sorbent, which can be expressed with respect to time:

$$\dot{m}_{cap} = \rho_a \times V \times \frac{d(Y_a)}{dt} \tag{15}$$

Similarly, the desorption and adsorption rates can be obtained using the following relations:

$$\text{Desorption rate} = \dot{m}_a(Y_{a\,f} - Y_{a\,i}) \tag{16}$$

$$\text{Adsorption rate} = \dot{m}_a(Y_{a\,i} - Y_{a\,f}) \tag{17}$$

The power consumed by the heater to heat the inlet air in the desorption process is calculated as follows:

$$\dot{W}_{heater} = \rho_a \times \dot{V} \times c_{p,a} \times (T_{reg} - T_{amb}) \tag{18}$$

where $\dot{V}$ is the volumetric flow rate, which is affected by air velocity and the air inlet section dimensions. A velocity range of 0.2 to 2.5 m/s can be considered for the appropriate reaction between the sorbent layers and the airflow.

The rejected heat from the condenser to distill the humid air is calculated from Eq. (19):

$$\begin{aligned}\dot{Q}_{cond} &= \dot{Q}_{sen} + \dot{Q}_{lat} \\ &= \left[(\rho AV)(C_p)(T_a - T_{dew}) \right. \\ &\qquad \left. + (\rho AV)(Y_a)(h_{cond})\right]\end{aligned} \tag{19}$$

It is worth noting that the moisture released in the desorption process is slightly less than the moisture adsorbed in the adsorption process due to the presence of chemical irreversibility. The efficiency of an ABAWH system depends on the efficiency of moisture condensation in the condenser and the efficiency of moisture desorption from the sorbent bed. It is obvious that the best performance of the system occurs when all the adsorbed moisture is desorbed from the sorbent and all the desorbed moisture is condensed.

Another factor known as water yield can be used to indicate how much water is produced with respect to the total energy consumption:

$$WY = \frac{\dot{m}_{cap}}{\dot{E}_{tot}} \tag{20}$$

The total energy consumption of the system is equal to the summation of the energy consumed by the heater and the condenser:

$$\begin{aligned}E_{tot} &= \left[\dot{m}_a c_p (T_{amb} - T_{reg})\right] \\ &\quad + \left[\dot{m}_a c_p (T_{a\,f} - T_{dew}) \right. \\ &\quad \left. + \dot{m}_a Y_{a\,f} h_{cond}\right]\end{aligned} \tag{21}$$

3. Results and Discussion

Fig. 5 indicates the simulation results of the desorption process in 600 seconds at an air velocity of 0.2 m/s. The decrease in the sorbent water uptake capacity shown in Fig. 5(a) demonstrates the release of moisture to the regenerative passing air. As a result, the air humidity ratio gradually increases. As seen in Fig. 5 (a), the sorbent water uptake capacity after 600 seconds has reached 0.14 kg_w/kg_s at the outlet, which displays a decrease of 0.03. This decrease will continue over time. However, it should be noted that the air temperature also increases, which leads to a decrease in the dew point temperature and an increase in the energy consumption by the condenser since the air humidity ratio will not change significantly after a short time. Therefore, there is no need to desorb the sorbent bed completely. Although more water will be generated as the desorption process becomes lengthier, the energy consumption will also increase and the system efficiency will drop.

During the desorption process, the dew point temperature of the passing air increases. As can be seen in Fig. 6, the air humidity ratio grew from approximately 0.093 kg_w/kg_a to 0.193 kg_w/kg_a, which caused the dew point temperature to grow from 12.8°C before entering the sorbent bed to a maximum of 25°C by the completion of the desorption process.

Fig. 7 shows the variation of air temperature and humidity ratio along the sorbent bed. The main variations occur at the beginning of the sorbent bed due to the relatively low thermal conductivity and mass diffusivity of the sorbent. Consequently, selecting an appropriate length for the sorbent bed is of primary importance.

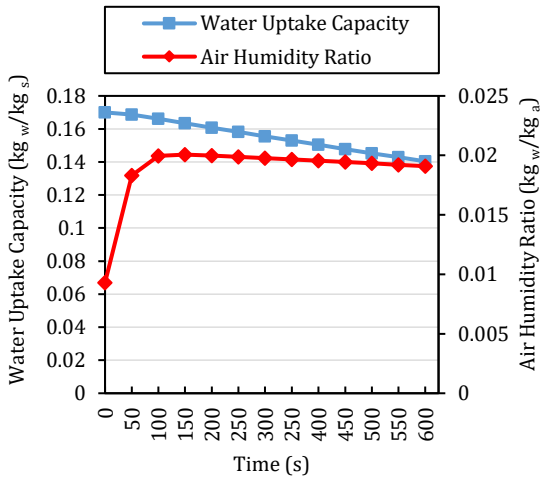

(a)

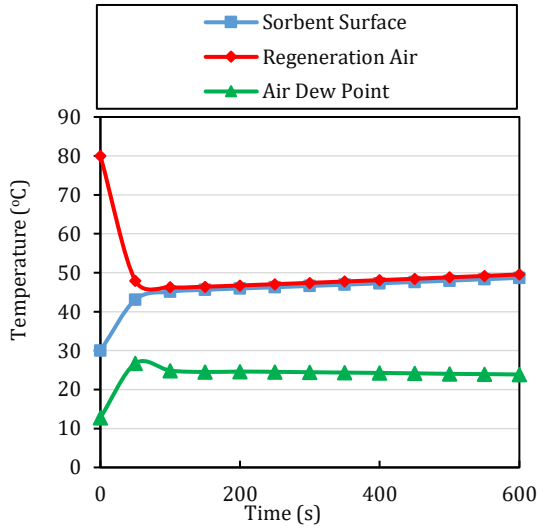

(b)

Fig. 5. Variation of the outlet (a) sorbent water uptake capacity (W) and air humidity ratio (Y_a) and (b) air temperature, sorbent temperature, and air dew point temperature

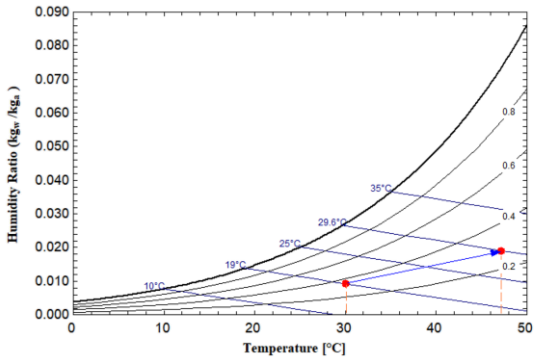

Fig. 6. Variation of air properties during regeneration

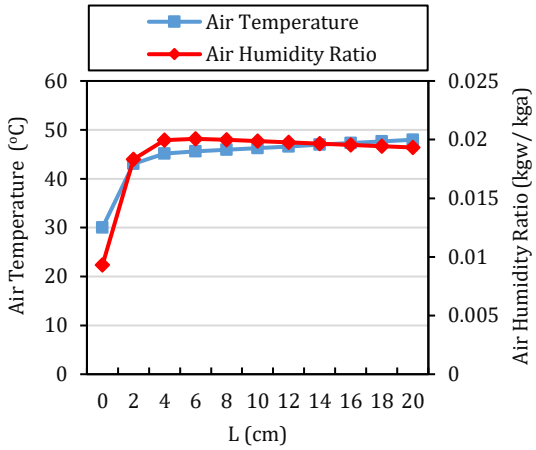

Fig. 7. Variation of air temperature and humidity ratio along the bed after 600 seconds

Fig. 8 (a) shows the difference between adsorption and desorption rates in a single sinusoidal channel. Unlike the desorption process, adsorption demands more time to complete, especially when the sorbent is saturated. Therefore, the air velocity in the adsorption process should be higher than in the desorption process. In other words, the air flow rate should be increased. According to the results of Fig. 8 (b), at the air velocity of 2.5 m/s, the time required to increase a capacity of 0.14 kg_w/kg_s to approximately 0.17 kg_w/kg_s is at least 3600 seconds. It is worth noting that the velocity should not exceed a limit such that the chemical reaction between the sorbent and the airflow does not occur. As several articles have mentioned [40, 41], the water uptake capacity of silica gel at 30°C and 35% relative humidity is less than 0.2 kg_w/kg_s. This was also obtained from the numerical simulation of the adsorption process. Fig. 8 (b) also illustrates that after 4000 seconds, the sorbent water uptake capacity is almost constant and does not exceed 0.17 kg_w/kg_s, which means that the sorbent is saturated and has no tendency to adsorb more moisture over time.

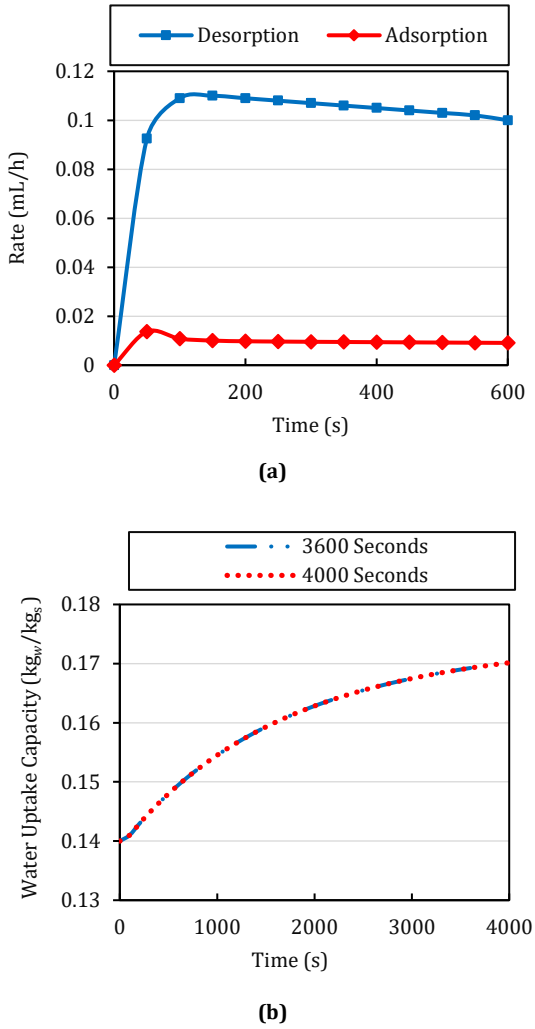

Fig. 8. Variations of (a) adsorption and desorption rates and (b) sorbent water uptake capacity over time

By knowing the cross-sectional area of each channel (control volume) and its number in the sorbent bed, the overall flow rate of the passing air in the desorption process is determined. Then, using the air humidity ratio (Y_a), the amount of water production can be calculated. Fig. 9 (a) shows the water production rate in one sinusoidal channel. The actual amount of generated water is lower than that shown in Fig. 9 (a) because the condenser efficiency in reality is not 100%. By assuming 100,000 channels in the sorbent bed (meaning a total cross-sectional area of 1.225 m^2), the average water production rate will be ideally 5.4 mL/s. As can be seen from Fig. 9 (a), the water production rate using the ABAWH method is significantly higher than that using the condenser directly without any sorbent beds. However, it should be noted that the air flowing through the sorbent bed does not only increase air moisture content but also results in an increase in temperature. Therefore, the system works effectively as long as there is a balance between the condenser energy consumption and the amount of water production. As Fig. 9 (b) indicates, with the gradual increase of the air temperature inside the sorbent bed, the difference between the air temperature and the dew point temperature increases. Such a temperature difference leads to higher energy consumption by the condenser.

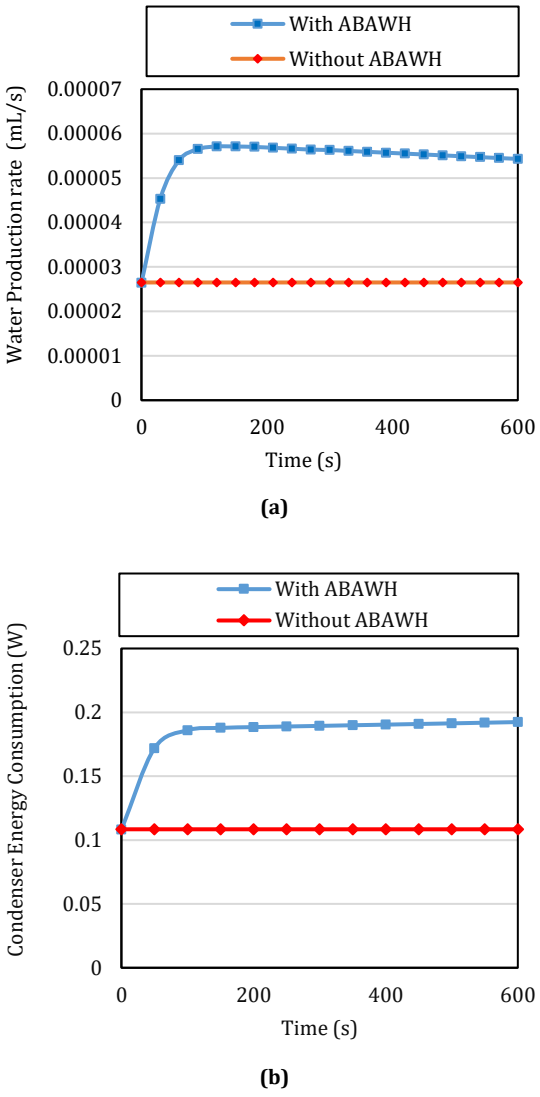

Fig. 9. (a) Water production rate from each channel in the desorption process and (b) condenser energy consumption with and without using ABAWH

3.1. Parametric Study

The performance improvement of the system or increase in water yield is obtained by increasing water production and reducing the condenser energy consumption. For this purpose, the dew point temperature should increase so that its difference with the ambient temperature diminishes and the condenser energy consumption decreases. In the following section, the impact of three parameters—sorbent water uptake capacity, air velocity, and regeneration temperature—on dew point temperature and air humidity ratio is investigated. The higher the

water uptake capacity of the sorbent, the more moisture it adsorbs from the flowing air; therefore, by using a sorbent with a higher capacity, the air humidity ratio increases to a greater extent in the desorption process. However, it should be noted that the water uptake capacity of sorbent depends on its structure and climatic conditions. Fig. 10 shows the effect of sorbent water uptake capacity on system performance. Using a sorbent with a higher water uptake capacity increases the water yield and the flowing air's humidity ratio.

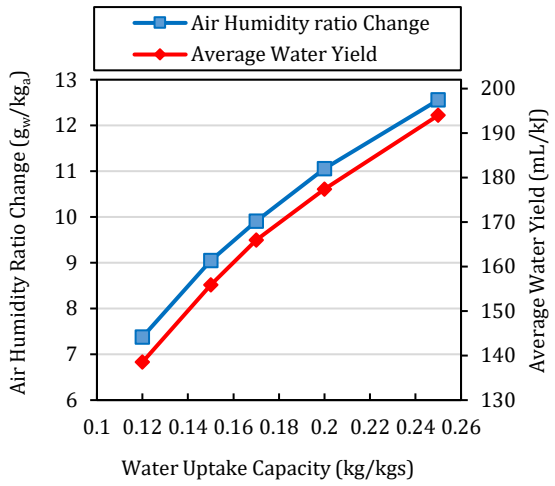

Fig. 10. Effect of sorbent water uptake capacity on the system performance

The regeneration temperature of the desorption process also plays an important role in the mass transfer mechanism and heat transfer rate. The higher the regeneration temperature, the higher the sorbent desorption rate, and the process of moisture release from the sorbent is enhanced. Fig. 11 shows that a higher regeneration temperature leads to an accelerated water uptake capacity reduction during the desorption process and the growth of the dew point temperature.

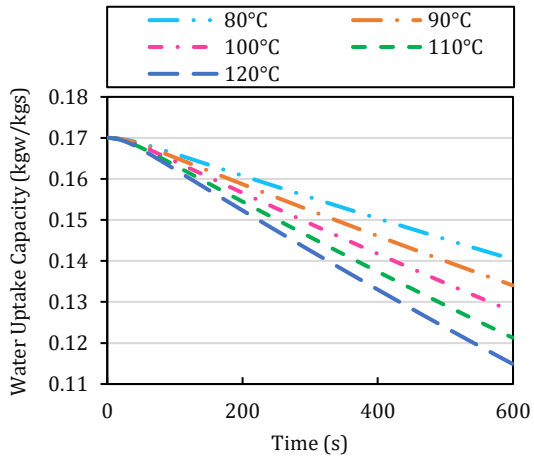

(a)

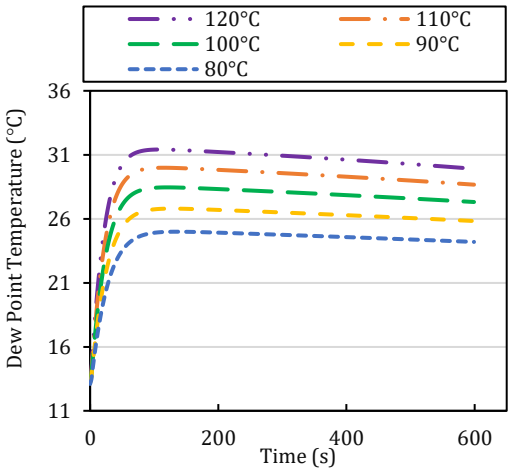

(b)

Fig. 11. Effect of regeneration temperature on (a) sorbent water uptake capacity and (b) dew point temperature at the sorbent bed outlet during the desorption process

Fig. 12 shows that the water yield decreases because more thermal energy is required to provide the regeneration temperature despite the increase in the sorbent desorption rate as the regeneration temperature increases. Also, the higher temperature difference between the airflow and the dew point leads to an increase in condenser energy consumption.

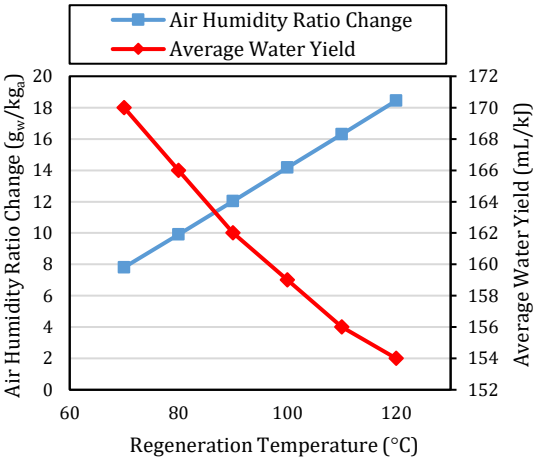

Fig. 12. Effect of regeneration temperature on the system performance

The velocity of the airflow passing through the sorbent layers is another crucial factor in the heat and mass transfer mechanism. Increasing the air velocity reduces the mass transfer time between air and sorbent, and on the other hand, improves heat transfer.

Fig. 13 (a) shows that the rate of air humidity ratio changes in the desorption process and the system water yield decreases after the velocity of 0.5 m/s. Fig. 13 (b) shows the effect of air velocity on the adsorption process during 100 seconds.

As mentioned earlier, increasing the airflow velocity slows down the mass transfer. However, a higher velocity contributes to a greater flow rate, which has a positive effect on the adsorption process, as it leads to the faster saturation of the sorbent layer.

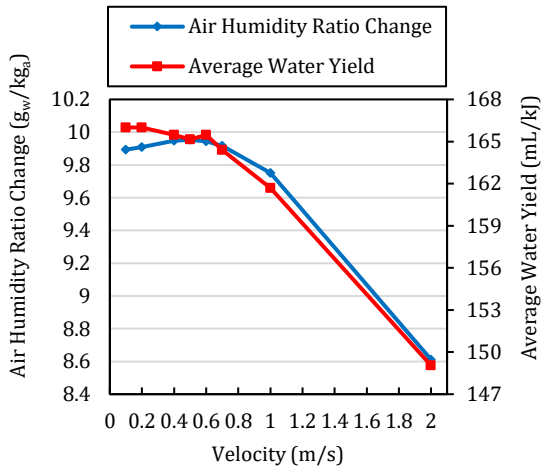

(a)

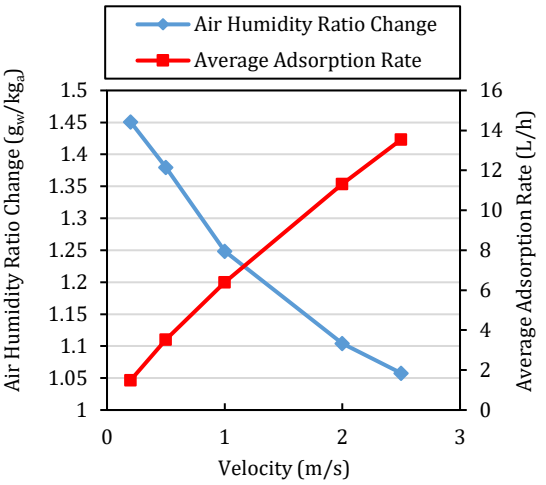

(b)

Fig. 13. Effect of air velocity on the proposed system performance (a) desorption process and (b) adsorption process

The average water yield of the system and desorption rate are also shown as a function of relative humidity in Fig. 14. It is found that by increasing the relative humidity of the test environment, both the desorption rate and air humidity ratio increase to a great extent. Furthermore, due to the higher moisture content, the system performance is also improved and with a given energy consumption, more water can be harvested.

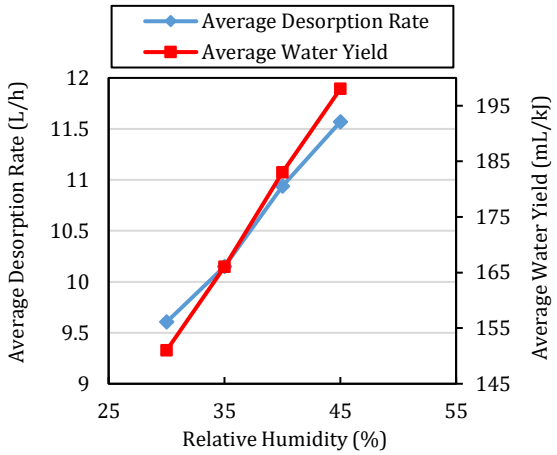

Fig. 14. Average desorption rate and water yield ratio during 600 seconds

For a better understanding of the system performance, a comparison between the water yield of the proposed technique and the case where the atmospheric air undergoes direct cooling in the condenser is shown in Fig. 15. It is observed that the use of the ABAWH system in arid areas is more cost-effective than that in humid areas. In arid areas, in addition to the low atmospheric moisture content, the difference between the air dew point temperature and the ambient temperature is higher, which leads to more energy consumption in the condenser. As a result, the water yield of the direct mode is significantly lower than that of the ABAWH device. However, with the increase of relative humidity, the difference between water yield ratios decreases. Fig. 15 also shows that in all relative humidity levels, the condenser energy consumption of an ABAWH device is higher than the cooling energy required for the direct distillation of air moisture, because the outlet of the sorbent bed is a humid airflow that contains more water than the atmospheric air; thus, more energy is needed to distill it.

Fig. 16 shows a comparison between the performance of the proposed system and a conventional mono-cycle ABAWH system which only carries out one single water production cycle per day. As shown in Fig. 16, the amount of water yield is higher in the proposed multi-cycle ABAWH compared to a mono-cycle system. A sorbent bed with a cross-sectional area of 1.225 m^2 can produce distilled water at a rate of 19440 mL/h, 31% higher than a single-cycle device.

Moreover, the time required for each water production cycle is longer in a conventional ABAWH system with one sorbent bed, because adsorption and desorption processes are not taking place simultaneously.

As suggested in this study, considering that the time required to carry out the adsorption and desorption processes is 3600 and 600 seconds respectively, the minimum amount of time needed to perform each water production cycle in a single bed device will be 4200 seconds, which results in a maximum of 10 cycles of water production in 12 hours of the day. On the other hand, by using two sorbent beds under the same conditions, the time for each will be one hour, which means a maximum of 12 cycles per day. Therefore, under the same conditions, the water production of the proposed and single-bed ABAWH are 38800 mL and 32400 mL, respectively.

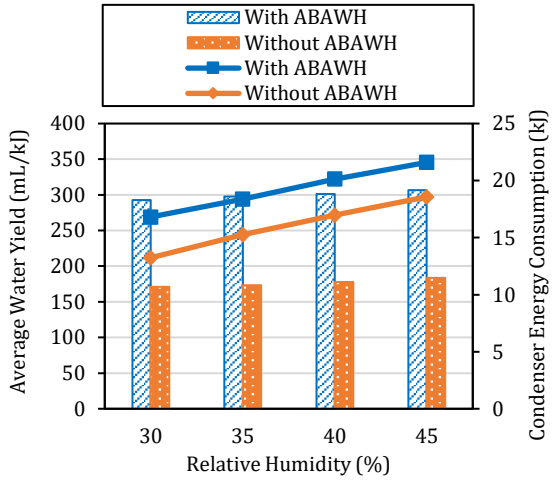

Fig. 15. System performance ratio and condenser energy consumption at different relative humidities

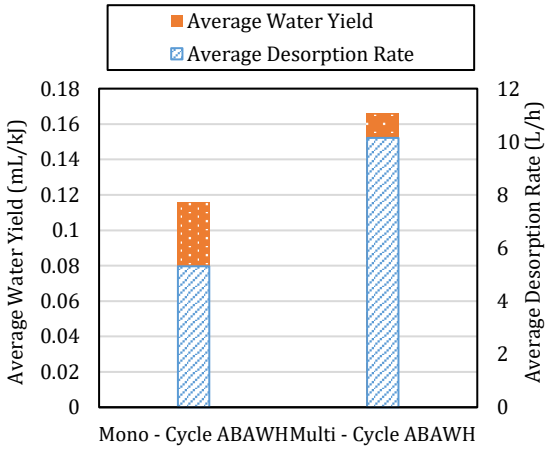

Fig. 16. Performance comparison between proposed and conventional mono-cycle ABAWH

4. Conclusions

In this study, a numerical simulation was conducted on the sorbent bed of a quasi-continuous active ABAWH system containing silica gel sorbent, at a temperature of 30 °C and a relative humidity of 35% (a relatively hot and dry climate). The results can be summarized as follows:

- In a relative humidity of 35%, the maximum water uptake capacity of the sorbent is 0.17 kg_w/kg_s. Beyond this point, continuing the adsorption process is not advantageous as the quantity of moisture absorbed remains constant. As a result, the optimum duration for the desorption process is 600 seconds, while the adsorption process should last for at least 3600 seconds.
- Under ideal conditions, disregarding any irreversibility, a sorbent bed with a cross-sectional area of 1.225 m^2 can produce distilled water at a rate of 19440 mL/h. This output is 31% higher than what a typical active system, operating one cycle per day, can generate.
- Neglecting the time needed for moisture condensation in the condenser and assuming that the system operates continuously, each water production cycle will take 60 minutes. This allows for approximately 12 cycles within 12 hours of the day, resulting in water production of 38800 mL or 31670 mL/m^2. The ABAWH system, with a single sorbent bed, can handle up to 10 cycles per day, yielding a maximum water output of 32400 mL.
- The average water yield of the proposed system under the relative humidity of 35% and regeneration temperature of 80 °C is 0.166 mL/kJ which is 43% higher than that of a mono-cycle system.

5. Future Recommendation

This study is the first to numerically simulate the dynamic behavior of adsorption and desorption to assess the feasibility of water production and establish an upper limit for its potential. Future research can enhance this numerical framework by incorporating the condensation process to provide a more comprehensive and realistic understanding. Additionally, further studies can explore the impact of different chemical properties of sorbents beyond silica gel and investigate alternative system designs to optimize performance and efficiency.

Nomenclature

a	Width of sorbent channel (m)
b	Height of sorbent channel (m)
c_p	Specific heat $(\frac{J}{kg.K})$

D_h	Hydraulic diameter (m)
D_s	Mass diffusivity $(\frac{m^2}{s})$
E	Energy (J)
f	Mass fraction of sorbent in bed
h	Convective heat transfer coefficient $(\frac{W}{m^2.K})$
h_m	Convective mass transfer coefficient $(\frac{kg}{m^2.s})$
k	Thermal conductivity $(\frac{W}{m.K})$
L	Length (m)
Le	Lewis number
$\dot{m}$	Mass flow rate $(\frac{kg}{s})$
Nu	Nusselt number
L	Length (m)
P	Pressure (Pa)
Q_{sor}	Sorption enthalpy (J)
$\dot{Q}$	Heat (W)
RH	Relative humidity
T	Temperature (°C)
t	Time (s)
u	Velocity $(\frac{m}{s})$
$\dot{V}$	Volumetric flow rate $(\frac{m^3}{s})$
w	Water uptake capacity $(\frac{kg\ (water)}{kg\ (sorbent)})$
Ẇ	Power (W)
WY	Water yield $(\frac{mL}{kJ})$
Y	Humidity ratio $(\frac{kg}{kg(dry\ air)})$
x	Longitudinal coordinate (m)

Greek symbols

α	Specific surface $(\frac{1}{m})$
ε	Porosity ratio
ρ	Density $(\frac{kg}{m^3})$
φ	Relative humidity

Subscripts

a	Air
amb	Ambient
$cond$	Condensation
dew	Dew point
f	Final
i	Initial
l	Liquid water
lat	Latent
p	process
reg	Regeneration
$sens$	Sensible
s	Sorbent
tot	Total
v	Water vapor
vap	Evaporation
vs	Saturation vapor
w	water

Funding Statement

This work was supported by a grant presented by the Vice Chancellor of Research of the Kharazmi University.

Conflicts of Interest

The authors declare that there is no conflict of interest regarding the publication of this article.

Maryam Karami, the corresponding author of this paper is the current Assistant Editor of Journal of Heat and Mass Transfer Research, but she has no involvement in the peer review process used to assess this work submitted to the Journal.

This paper was assessed, and the corresponding peer review managed by another Assistant Editor of Journal.

Authors Contribution Statement

Zahra Piryaei: Conceptualization; Formal Analysis; Investigation; Methodology, Validation; Writing – Original Draft;
Aryan Jouneghaninaseri: Investigation; Methodology; Data Curation;
Maryam Karami: Conceptualization; Project administration; Supervision; Writing – Review & Editing.

References

[1] Raveesh, G., Goyal, R. & Tyagi, S. K., 2025. Sugarcane bagasse derived composite sorbent for sorption based atmospheric water harvesting. *Separation and Purification Technology*, 356, 129820.

[2] Wang, M., Liu, E., Jin, T., Zafar, S.-U., Mei, X., Fauconnier, M.-L. & De Clerck, C., 2024. Towards a better understanding of atmospheric water harvesting (AWH) technology. *Water Research*, 250, 121052.

[3] Agrawal, A. & Kumar, A., 2024. A comprehensive review of fresh water

production from atmospheric air – techniques, challenges and opportunities. *Environment, Development and Sustainability*, pp.1-36.

[4] Ehtisham, M., Saeed-ul-hassan, M. & Poater, A., 2025. A comprehensive review of approaches, systems, and materials used in adsorption-based atmospheric water harvesting. *Science of The Total Environment*, 958, 177885.

[5] Xu, W. & Yaghi, O. M., 2020. Metal–organic frameworks for water harvesting from air, anywhere, anytime. *ACS central science*, 6, 1348-1354.

[6] Almassad, H. A., Abaza, R. I., Siwwan, L., AL-Maythalony, B. & Cordova, K. E., 2022. Environmentally adaptive MOF-based device enables continuous self-optimizing atmospheric water harvesting. *Nature communications*, 13, 4873.

[7] Ejeian, M. & Wang, R., 2021. Adsorption-based atmospheric water harvesting. *Joule*, 5, 1678-1703.

[8] Tashtoush, B. & Alshoubaki, A., 2023. Atmospheric water harvesting: A review of techniques, performance, renewable energy solutions, and feasibility. *Energy*, 128186.

[9] Karami, M. & Nasiri Gahraz, S. S., 2022. Improving thermal performance of a solar thermal/desalination combisystem using nano fluid-based direct absorption solar collector. *Scientia Iranica*, 29, 1288-1300.

[10] Karami, M. & Nasiri Gahraz, S. S., 2021. Transient simulation and life cycle cost analysis of a solar polygeneration system using photovoltaic-thermal collectors and hybrid desalination unit. *Journal of Heat and Mass Transfer Research*, 8, 243-256.

[11] Alkhudhiri, A., Darwish, N. & Hilal, N., 2012. Membrane distillation: A comprehensive review. *Desalination*, 287, 2-18.

[12] Kim, H., Rao, S. R., Kapustin, E. A., Zhao, L., Yang, S., Yaghi, O. M. & Wang, E. N., 2018. Adsorption-based atmospheric water harvesting device for arid climates. *Nature communications*, 9, 1191.

[13] Kim, H., Yang, S., Rao, S. R., Narayanan, S., Kapustin, E. A., Furukawa, H., Umans, A. S., Yaghi, O. M. & Wang, E. N., 2017. Water harvesting from air with metal-organic frameworks powered by natural sunlight. *Science*, 356, 430-434.

[14] Hanikel, N., Prévot, M. S., Fathieh, F., Kapustin, E. A., Lyu, H., Wang, H., Diercks, N. J., Glover, T. G. & Yaghi, O. M., 2019. Rapid cycling and exceptional yield in a metal-organic framework water harvester. *ACS central science*, 5, 1699-1706.

[15] Fathieh, F., Kalmutzki, M. J., Kapustin, E. A., Waller, P. J., Yang, J. & Yaghi, O. M., 2018. Practical water production from desert air. *Science advances*, 4, eaat3198.

[16] Ejeian, M., Entezari, A. & Wang, R., 2020. Solar powered atmospheric water harvesting with enhanced LiCl/MgSO4/ACF composite. *Applied Thermal Engineering*, 176, 115396.

[17] Sleiti, A. K., Al-Khawaja, H., Al-Khawaja, H. & Al-Ali, M., 2021. Harvesting water from air using adsorption material–Prototype and experimental results. *Separation and Purification Technology*, 257, 117921.

[18] Kumar, P. M., Arunthathi, S., Prasanth, S. J., Aswin, T., Antony, A. A., Daniel, D., Mohankumar, D. & Babu, P. N., 2021. Investigation on a desiccant based solar water recuperator for generating water from atmospheric air. *Materials Today: Proceedings*, 45, 7881-7884.

[19] Kumar, M. & Yadav, A., 2015. Experimental investigation of design parameters of solar glass desiccant box type system for water production from atmospheric air. *Journal of Renewable and Sustainable Energy*, 7.

[20] Essa, F., Elsheikh, A. H., Sathyamurthy, R., Manokar, A. M., Kandeal, A., Shanmugan, S., Kabeel, A., Sharshir, S. W., Panchal, H. & Younes, M., 2020. Extracting water content from the ambient air in a double-slope half-cylindrical basin solar still using silica gel under Egyptian conditions. *Sustainable Energy Technologies and Assessments*, 39, 100712.

[21] Srivastava, S. & Yadav, A., 2018. Water generation from atmospheric air by using composite desiccant material through fixed focus concentrating solar thermal power. *Solar Energy*, 169, 302-315.

[22] Elashmawy, M. & Alshammari, F., 2020. Atmospheric water harvesting from low humid regions using tubular solar still powered by a parabolic concentrator system. *Journal of Cleaner Production*, 256, 120329.

[23] Fathy, M. H., Awad, M. M., Zeidan, E.-S. B. & Hamed, A. M., 2020. Solar powered foldable apparatus for extracting water from atmospheric air. *Renewable energy*, 162, 1462-1489.

[24] Wang, X., Li, X., Liu, G., Li, J., Hu, X., Xu, N., Zhao, W., Zhu, B. & Zhu, J., 2019. An interfacial solar heating assisted liquid sorbent atmospheric water generator. *Angewandte Chemie*, 131, 12182-12186.

[25] LaPotin, A., Zhong, Y., Zhang, L., Zhao, L., Leroy, A., Kim, H., Rao, S. R. & Wang, E. N., 2021. Dual-stage atmospheric water harvesting device for scalable solar-driven water production. *Joule*, 5, 166-182.

[26] Raveesh, G., Goyal, R. & Tyagi, S. K., 2025. Sugarcane bagasse derived composite sorbent for sorption based atmospheric water harvesting. *Separation and Purification Technology*, 356, 129820.

[27] Li, R., Shi, Y., Wu, M., Hong, S. & Wang, P., 2020. Improving atmospheric water production yield: Enabling multiple water harvesting cycles with nano sorbent. *Nano energy*, 67, 104255.

[28] Wang, J., Wang, R., Tu, Y. & Wang, L., 2018. Universal scalable sorption-based atmosphere water harvesting. *Energy*, 165, 387-395.

[29] Wang, J., Liu, J., Wang, R. & Wang, L., 2017. Experimental investigation on two solar-driven sorption based devices to extract fresh water from atmosphere. *Applied Thermal Engineering*, 127, 1608-1616.

[30] Agrawal, A. & Kumar, A., 2025. Experimental comparison and 6E analyses of double-ended evacuated tube collector based atmospheric water harvesting with and without PCM. *Solar Energy Materials and Solar Cells*, 282, 113343.

[31] Agrawal, A. & Kumar, A., 2024. Experimental comparison of solar-powered adsorption-based atmospheric water harvesting using air-to-air & water-to-air heat exchanger for condensation. *Environmental Progress & Sustainable Energy*, 43.

[32] Agrawal, A. & Kumar, A., 2024. Double-ended vacuum tube collector based solar powered atmospheric water harvesting by using composite desiccant material 'Jute/$CaCl_2$'. *Energy Sources, Part A: Recovery, Utilization, and Environmental Effects*, 46, 9972-9993.

[33] Kang, H., Lee, G. & Lee, D.-Y., 2015. Explicit analytic solution for heat and mass transfer in a desiccant wheel using a simplified model. *Energy*, 93, 2559-2567.

[34] Chung, J. D., Lee, D.-Y. & Yoon, S. M., 2009. Optimization of desiccant wheel speed and area ratio of regeneration to dehumidification as a function of regeneration temperature. *Solar Energy*, 83, 625-635.

[35] Chung, J. D., 2017. Modeling and analysis of desiccant wheel. *Desiccant Heating, Ventilating, and Air-Conditioning Systems*, 11-62.

[36] Nia, F. E., Van Paassen, D. & Saidi, M. H., 2006. Modeling and simulation of desiccant wheel for air conditioning. *Energy and buildings*, 38, 1230-1239.

[37] Heidarinejad, G. & Pasdarshahri, H., 2010. The effects of operational conditions of the desiccant wheel on the performance of desiccant cooling cycles. *Energy and Buildings*, 42, 2416-2423.

[38] Harshe, Y. M., Utikar, R. P., Ranade, V. V. & Pahwa, D., 2005. Modeling of rotary desiccant wheels. *Chemical Engineering & Technology: Industrial Chemistry-Plant Equipment-Process Engineering-Biotechnology*, 28, 1473-1479.

[39] Zhang, L. & Niu, J., 2002. Performance comparisons of desiccant wheels for air dehumidification and enthalpy recovery. *Applied Thermal Engineering*, 22, 1347-1367.

[40] NG, K. C., CHUA, H., CHUNG, C., LOKE, C., KASHIWAGI, T., AKISAWA, A. & SAHA, B. B., 2001. Experimental investigation of the silica gel–water adsorption isotherm characteristics. *Applied Thermal Engineering*, 21, 1631-1642.

[41] Riffel, D. B., Schmidt, F. P., Belo, F. A., Leite, A. P., Cortés, F. B., Chejne, F. & Ziegler, F., 2011. Adsorption of water on Grace Silica Gel 127B at low and high pressure. *Adsorption*, 17, 977-984.